

Article

Effects of Pre-Deformation under Tension and Annealing Process on the Microstructure and Properties of Al-6Mg-1.0Mn Extruded Wide Reinforcement Plate

Pengwei Li ^{1,2}, Qiqiang Han ², Wei Sun ^{1,2}, Xiangjie Wang ^{1,*}, Jianzhong Cui ¹, Rui Wang ², Chunzhong Liu ³ and Min Jiang ^{1,*}

¹ Key Lab of Electromagnetic Processing of Materials, Ministry of Education, Northeastern University, Shenyang 110819, China

² Zhongwang Group Co., Ltd., Liaoyang 111003, China

³ School of Material Science and Engineering, Shenyang Aerospace University, Shenyang 110136, China

* Correspondence: wangxj@epm.neu.edu.cn (X.W.); jiangm@smm.neu.edu.cn (M.J.)

Abstract: In order to achieve the combination of mechanical and corrosion properties for the Al-Mg-Mn alloy, a novel combination of pre-deformation under tension and an annealing process was investigated on the microstructure and properties of the Al-6Mg-1.0Mn extruded wide reinforcing plate. This was conducted by means of a tensile test, an intergranular corrosion test, scanning electron microscopy (SEM), and transmission electron microscope (TEM) experiments. The results showed that when the pre-deformation under tension in the range of 10–14%, the corrosion performance is first decreased, and then increases with the increase in temperature, becoming stable at 300 °C. After stabilization annealing at 300 °C for 2 h and then sensitizing at 150 °C for 10–200 h, the intergranular corrosion resistance of the aluminum alloy first decreases and then increases as the sensitization time is prolonged. When the sensitization time exceeds 50 h, the intergranular corrosion resistance is significantly improved. After 14% pretension and stabilization annealing at 300 °C for 2 h, the tensile strength, yield strength, and elongation of the alloy reached 360 MPa, 205 MPa, and 18.5%, and a good combination of strength and corrosion resistance of Al-Mg-Mn alloys could be obtained. These excellent properties were attributed to the continuous distribution of β -phase at the grain boundaries, and the combination of pre-deformation under tension with the annealing process promotes the dynamic precipitation of nanoparticles and the formation of substructure.

Keywords: Al-6Mg-1.0Mn aluminum alloys; pre-deformation under tension; annealing; intergranular corrosion; extruded wide strip reinforcing plate



Citation: Li, P.; Han, Q.; Sun, W.; Wang, X.; Cui, J.; Wang, R.; Liu, C.; Jiang, M. Effects of Pre-Deformation under Tension and Annealing Process on the Microstructure and Properties of Al-6Mg-1.0Mn Extruded Wide Reinforcement Plate. *Crystals* **2022**, *12*, 1415. <https://doi.org/10.3390/cryst12101415>

Academic Editor: Indrajit Charit

Received: 7 September 2022

Accepted: 29 September 2022

Published: 6 October 2022

Publisher's Note: MDPI stays neutral with regard to jurisdictional claims in published maps and institutional affiliations.



Copyright: © 2022 by the authors. Licensee MDPI, Basel, Switzerland. This article is an open access article distributed under the terms and conditions of the Creative Commons Attribution (CC BY) license (<https://creativecommons.org/licenses/by/4.0/>).

1. Introduction

Al-Mg alloys with medium strength, excellent welding properties, and corrosion resistance are widely used in industrial fields such as aviation and shipping, as extruded strip plates have been used in the manufacture of the structural parts of ship hulls in recent years [1–3]. With the rapid development of China's high-tech equipment, the material requirements for aviation and marine applications are also increasingly high. In order to avoid repeated welding caused by a decline in strength and corrosion resistance, extrusion of a 1600 mm ultra-wide strip reinforcement plate has become the development trend. At present, a 5083 (Mg: 4.0–4.9%) alloy is widely used in the field of marine strip plates. This alloy has good corrosion resistance and welding performance, but relatively low strength. The 5A06 alloy (Mg: 5.8–6.8%), which was subsequently developed in the former Soviet Union, has enhanced strength compared with 5083 due to the increase in Mg content, resulting in enhanced solid solution strengthening [4–6]. However, with the increase in Mg content, the thermal cracking tendency of aluminum alloy extrusion profiles increases. Mn is one of the key alloying elements in Al-Mg-based alloys, and enhances

their mechanical properties by dispersion strengthening and solid solution hardening. Mn is typically added to Al-Mg-based alloys to compensate for the negative effects of Fe [7]. It can also effectively prevent the growth of grains and increase the solution temperature of the alloy, so as to achieve the purpose of fully re-dissolving in the aluminum alloy solution treatment process. This increases the recrystallization temperature, and at the same time reduces the hot cracking tendency of extruded profiles [8,9]. Guo et al. reported the effect of pre-treatment combined with aging on the Al-Mg-Ag alloy's microstructure and mechanical properties. Results showed that thermomechanical treatment technology could effectively tune the precipitates and promote the formation of multiple nanostructures, such as sub-grains and cellular networks [10,11]. Thermomechanical treatment is an effective method for improving the strength of heat-treatable aluminum alloys, but the strength of the non-heat-treatable aluminum alloys is mainly improved by work hardening [12–15]. Numerous defects, such as dislocations, are generated during pre-deformation under tension. These defects can interact with precipitates in the post-aging process and improve the strength of the alloy significantly. However, due to the supersaturation of Mg, extended exposure to elevated service temperatures (as low as 40–50 °C) can cause precipitation of the intergranular β phase (Al_3Mg_2) in a process known as sensitization. Thus, without final stabilization annealing, the alloy properties are not stable and age softening will occur at room temperature [16]. Stabilization annealing will result in a more uniform distribution of β -phase, which in turn leads to stable mechanical properties and good corrosion resistance [17,18]. Intergranular corrosion (IGC) of Al-Mg-Mn alloys in the rolled and heat-treated states has been studied, but the effect of pre-deformation under tension and annealing processes on the combination of mechanical and corrosion properties of the Al-Mg-Mn alloy has rarely been reported on, to the best of our knowledge.

In high Mg Al-Mg-Mn alloys, the β -phase precipitates continuously in the grain boundaries at annealing temperatures of 150–220 °C [19]. The sensitization treatment temperatures were also selected within this interval, with 150 °C and 175 °C mostly used for sensitization treatments [20,21]. The pre-deformation under tension and annealing processes can tune the distribution of precipitates, and the IGC can be affected by the evolution of grain boundary precipitates (GBPs). This paper uses the mass loss method to analyze and evaluate intergranular corrosion. The sensitization test was also performed on the Al-Mg-Mn alloy in order to increase its susceptibility to intergranular corrosion, with the aim of investigating the precipitation characteristics of the β -phase and MnAl_6 phases during the annealing process of the Al-Mg-Mn alloy. The sensitization treatment in this paper aims to study the effect of long-term stabilization annealing on the phase precipitation pattern and intergranular corrosion properties. This paper investigated the effects of pre-deformation under tension as well as the annealing process on the microstructure and properties of an Al-6Mg-1.0Mn extruded wide reinforcing plate. This provides a theoretical basis for obtaining a wider strip plate with higher strength and intergranular corrosion resistance for mass production and application.

2. Experimental Materials and Methods

2.1. Material Preparation

The Al-Mg-Mn alloy extruded strip plate is produced by the 225 MN single-action horizontal extruder. The extruded billet is a hollow ingot with an outer diameter of 782 mm and an inner diameter of 550 mm. The expanded width of the wide extruded ribbed plate is 1750 mm. The material is extruded as a round tube, then cut, flattened, and corrected for size. The chemical composition is listed in Table 1. The profile processing process consists of the following: profile extrusion → pre-deformation under tension (an industrial-specific stretching machine is used along with special tooling to set the stretching length of the stretching machine in the deformation area, according to the stretching ratio of 5%, 10%, 14%, and 18%, then the ribbed plate is stretched and deformed) → stabilization annealing at 110, 150, 175, 220, 260, 300, 360 °C for 2 h. The production process parameters of the preparation process are shown in Table 2. The sensitization test uses an Al-Mg-Mn extruded

wide strip reinforcement plate in stabilization treatment at 300 °C for 2 h, then follows sensitization treatment at 150 °C for 10, 50, 100, and 200 h.

Table 1. Chemical composition of the Al-Mg-Mn strip reinforcing plate (wt.%).

Alloy	Si	Fe	Cu	Mn	Mg	Ti	Zr	Zn	Al
Al-Mg-Mn	0.05	0.13	0.01	1.0	6.0	0.08	0.06	0.02	Bal.

Table 2. Extrusion process parameters of the Al-Mg-Mn strip reinforcing plate.

Alloy	The Heating Temperature of Ingot/°C	Extrusion Speed/m/min	Temperature into the Quenching Zone/°C	Quenching Method	Temperature after Quenching/°C
Al-Mg-Mn	400–420	0.6	350	Air-cooled	<110

2.2. Microstructure Characterization

The microstructures were investigated with the Imager.M2m (Zeiss Optical Instruments, Shanghai International Trade, Germany) optical microscopy (OM), ultra-plus SSX-550 type SEM, equipped with an energy dispersive spectrometer (EDS). The OM and SEM samples were polished and etched with a mixture of nitric acid, hydrofluoric acid, hydrochloric acid, and distilled water. TEM measurements were carried out on a Tecnai G20 with an acceleration voltage of 200 kV. The TEM samples were mechanically polished to approximately 60 µm; then, a twin-jet electron-polishing technique was used to prepare the TEM samples at −30 °C in the electrolyte of HNO₃:CH₃OH = 1:3. During electro-polishing, a constant voltage of 25 V was adopted.

2.3. Mechanical Testing

Tensile specimens with a gauge length of 50 mm (extruding direction (ED)), a width of 12.5 mm (transverse direction (TD)), and a thickness of 2 mm were carried out on a CSS-44100 type universal testing machine, following the ASTM E8-04 standard. The testing was performed at room temperature. The initial strain rate was $1 \times 10^{-3} \text{ s}^{-1}$. Three parallel samples were tested to ensure reliability.

2.4. IGC Testing

The intergranular corrosion of the Al-Mg-Mn aluminum alloy strip plate was tested using nitric acid mass loss testing (NAMLT) following the ASTM G67-04 standard [22]. The size of each sample was 50 mm (ED) × 6 mm (TD) × 2 mm (normal direction (ND)). Each sample was artificially sensitized at 150 °C for 10, 50, 100, and 200 h. The reproduced samples of each preparation process condition were measured in conformity with the standard ASTM G67 for measuring the degree of sensitization through the nitric acid mass loss test. The intergranular damage was evaluated by examination of the transverse section (ND × TD) and extruding surface (ED × TD) of corroded samples.

In order to observe the depth of IGC, IGC testing was performed according to GB/T 7998-2005 standards using a reagent which included 10 mL H₂O₂ and 57 g NaCl in 1000 mL water [23]. Three specimens of each alloy, with a size of 40 × 25 × 2 mm³, are constantly immersed in standard IGC electrolytes at the test temperature, which was controlled at 35 ± 2 °C for 24 h. Three repeats were adopted for each condition. Both the surface and the cross sections after polishing are characterized by OM and SEM, the latter of which is also utilized to capture the maximum depth of the IGC.

3. Results and Analysis

3.1. Resistance to Intergranular Corrosion and Tensile Properties of Al-Mg-Mn Strip Plates after Stabilized Annealing

According to the ASTM G67 standard, the sensitivity of the sensitized alloys' corrosion depth and NAMLTL results are shown in Figure 1. If the NAMLTL value is less than or equal to 15 mg/cm^2 , the alloy is determined as resistant to IGC. When the NAMLTL is greater than or equal to 25 mg/cm^2 , the material can be regarded as susceptible to IGC. In order to further compare the IGC resistance after stabilization annealing, the cross-sections of the Al-Mg-Mn strip reinforcement plate were observed using an OM. It can be seen by the stabilization of the annealing samples at $110^\circ\text{C}/2 \text{ h}$ that they have a better intergranular corrosion resistance than $220^\circ\text{C}/2 \text{ h}$. The intergranular corrosion resistance increases and then decreases with the increase in pre-deformation under tension, and the best intergranular corrosion resistance of the Al-Mg-Mn strip plate is achieved when the pre-deformation under tension reaches 10% and 14%.

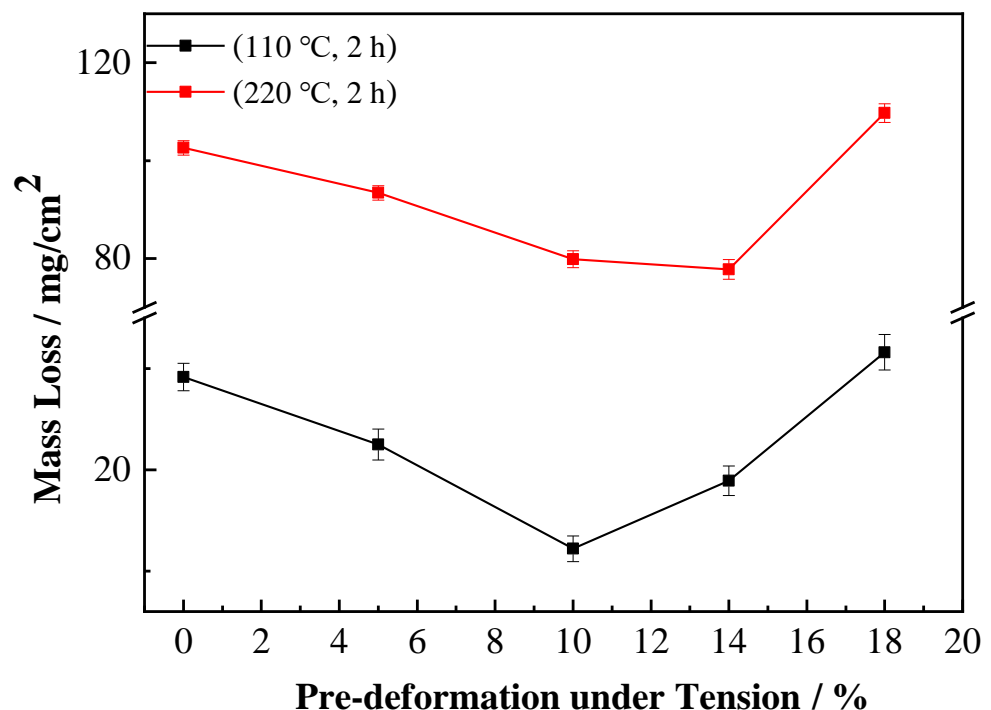


Figure 1. Influence of pre-deformation under tension on the quality weight of intergranular corrosion for Al-Mg-Mn strip reinforcement plate.

In order to verify the mass loss results of the investigated alloy, typical cross-sectional (ND \times TD) observations of corroded samples after the NAMLTL were investigated. Figure 2 shows the representative intergranular corrosion morphology corresponding to the intergranular corrosion mass loss under different regimes. Figure 2a,c,e show the intergranular corrosion profiles at 110°C for 2 h of the annealing regime, after 10%, 14%, and 18% pre-stretching, respectively. It can be observed that there is no obvious intergranular corrosion on the surface of the profile when the stretching amount is 10% and 14%. After stabilized annealing at 220°C for 2 h, typical intergranular corrosion morphology appears, as shown in Figure 2b,d,f, while the surface of Figure 3f appears to be peeling off. It can also be seen from Figure 1 that the pre-deformation under different tension amounts of two stabilized annealing regimes have the same pattern of influence on the intergranular corrosion properties. Figure 2g,h,i show the corroded morphologies of the surface (RD \times TD) of the ribbed plate after the NAMLTL test. It can be observed that the depth of the intergranular corrosion increases from $252.57 \mu\text{m}$ to $301.68 \mu\text{m}$ with the increase in

pre-deformation under tension. This also indicates that the IGC resistance of the alloy is greatly affected by the pre-deformation under tension and the annealing process.



Figure 2. Intergranular corrosion morphology and typical cross-sectional (ND × TD) observations after NAMLT test of the Al-Mg-Mn strip reinforcement plate alloy. (a) 10%-110 °C/2 h; (b) 10%-220 °C/2 h; (c) 14%-110 °C/2 h; (d) 14%-220 °C/2 h; (e) 18%-110 °C/2 h; (f) 18%-220 °C/2 h; (g) the intergranular corrosion diagram of (b); (h) the intergranular corrosion diagram of (d); (i) the intergranular corrosion diagram of (f).

Next, the better intergranular corrosion performance of the pre-deformation under tension is selected for the purpose of different temperature annealing, and then the best stabilization annealing system for sensitization is also selected. The NAMLT results shown in Figure 3 demonstrate the influence of the stabilization annealing temperature and sensitization time on intergranular corrosion properties. Figure 3a shows the pre-deformation under tension in 10% and 14%, annealed at different temperatures for 2 h. When the stabilization annealing temperature was below 220 °C, the corrosion resistance gradually deteriorated with the increasing stabilization annealing temperature, and the pre-deformation under tension of 14% was more easily corroded than 10%. When the stabilization annealing

temperature reached 220 °C, the worst intergranular corrosion performance was observed; while the stabilization temperature continued to increase toward 260 °C, the intergranular corrosion performance increased sharply. It can be seen that the best intergranular corrosion performance occurs at 300 °C for stabilization annealing. The pre-deformation under tension at 10% and 14% of the plate stabilization annealing at 300 °C for 2 h, followed by sensitization treatment at 150 °C for 10–200 h, is shown in Figure 3b. It can be observed that the high-temperature stabilization annealing state pre-deformation under tension 14% is better than at 10%. When the sensitization time increased to 50 h, the intergranular corrosion quality loss was the largest. When the sensitization time increased to 100 h, the intergranular corrosion stabilized, and the corrosion resistance was better. The optical microstructure in Figure 3 agrees with the results of the NAMLT test (Figure 2).

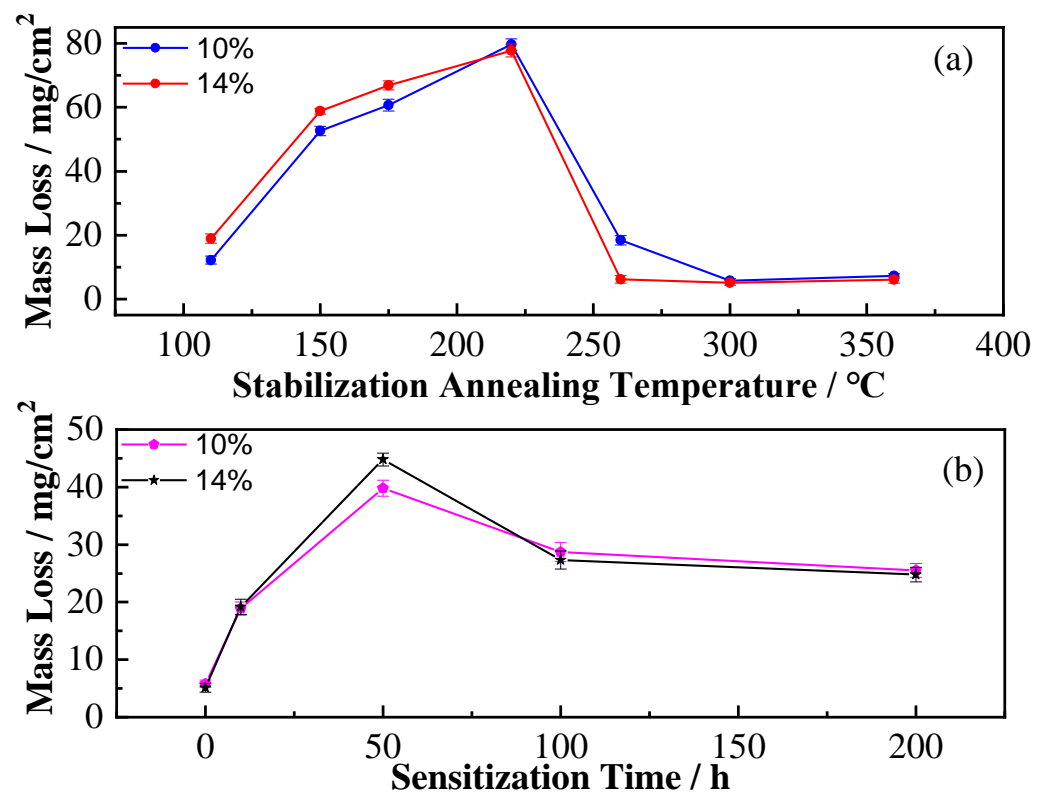


Figure 3. Influence of stabilization annealing temperature and sensitization time on the intergranular corrosion property. (a) the influence of stabilization annealing temperature and mass loss when the pre-deformation under tension is 10% and 14%; (b) the influence of stabilization time and mass loss when the pre-deformation under tension is 10% and 14%.

The influence of the stabilization annealing temperature on the mechanical properties of the investigated Al-Mg-Mn strip reinforcing plate is shown in Figure 4. In the subsequent stabilization annealing process, it became obvious that the Al-Mg-Mn properties have different degrees of recovery, and the pre-deformation under tension with amounts of 10% and 14% have the same trend. When the alloy was annealed for 2 h at 300 °C after 14% pre-deformation under tension, the ultimate tensile strength (UTS), yield strength (YS), and elongation of the alloy were 360 MPa, 205 MPa, and 18.5%, respectively. This far exceeds the performance requirements of ribbed plates in the marine field.

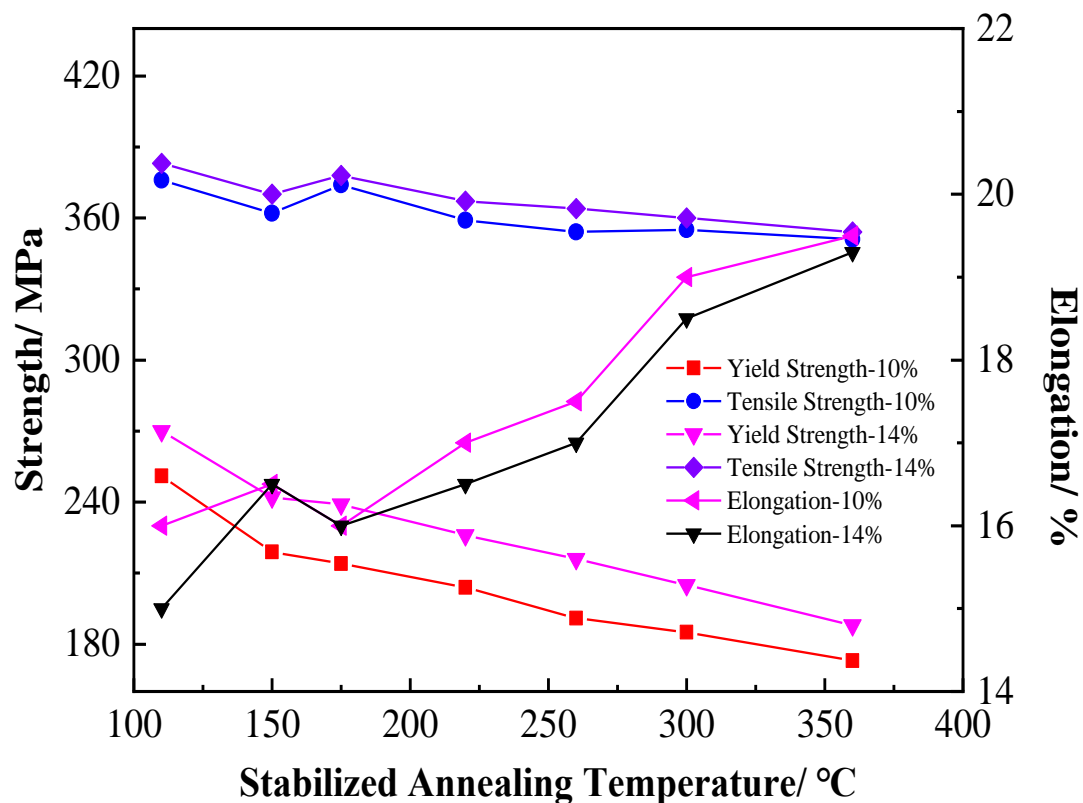


Figure 4. Mechanical property of Al-Mg-Mn strip reinforcement plate after annealing at different temperatures.

3.2. The Microstructure of Al-Mg-Mn Strip Plate with Pre-Deformation under Tension

The microstructure after stabilization annealing was observed by SEM. Figure 5 shows the microstructure after stabilization annealing of Al-Mg-Mn strip plates with different pre-deformations under tension. After 10% pre-deformation under tension of Al-Mg-Mn strip plate stabilization annealing at 110 °C for 2 h, a large number of short rod-like phases precipitated, accompanied by a small number of sphere-like phases with more uniform distribution. The length of these short rod-like phases was about 500 nm, as shown in Figure 5a. The Al-Mg-Mn strip plate with 14% pre-stretch pre-deformation under tension was stabilized and annealed at 110 °C for 2 h. Most of the precipitated phases were ellipsoidal, with a small amount of short rod-like phases. The size of the precipitated phases was larger than those of the 10% pre-deformation under tension, as shown in Figure 5d. After the 10% and 14% pre-deformation under tension of the plate stabilization annealing at 220 °C for 2 h, many continuous short rod-like phases precipitated on the grain boundary, and many spherical second phases precipitated in the crystal. With the increase in annealing temperature, the phases on the grain boundaries underwent tempering, and a small amount of phases grew and aggregated.

Electrochemical corrosion is the main form of intergranular corrosion of aluminum alloys. The main reason for this is that the precipitation phase is different from the matrix and the depletion zone near the grain boundary. Usually, the grain acts as the cathode, and impurities as well as alloying elements are mainly enriched on the grain boundary. The grain boundary is more active than the grain itself, and thus it becomes the anode and constitutes a micro corrosion cell, which produces corrosion along the grain boundary [24,25]. The TEM organization of the ribbed plate, with 14% pre-deformation under tension and annealing at different temperatures, is shown in Figure 6. As can be seen from the figure, all of the grains are elongated along the stretching direction. When annealing at 120 °C for 2 h, there is a large amount of cellular organization inside the alloy, as well as a large

amount of dislocation walls and a strong stress field (Figure 6a). When annealing at 220 °C for 2 h, the dislocations gradually move from the inside to the sides, and the dislocations with different numbers move above the cell wall. The dislocations inside the cell wall tissue gradually move to the cell wall and cancel out with the dislocations above the cell wall, which reduces the dislocation density and causes the dislocations to become regular. They are then rearranged near the grain boundary, forming a clearer cellular substructure. When annealing at 300 °C for 2 h, the cell wall becomes very thin and the dislocations are heavily reduced, at which time the presence of sphere-like and elongated second-phase particles can be clearly seen near the cell wall, pinned near the grain boundaries (Figure 6c). Further increasing the annealing temperature to 360 °C, the low temperature recovery area and cellular substructure is more obvious. The formation of orientations of different subgrain boundaries and sizes of sub-crystals is extremely uneven, and it was found that the dislocation also split the grain into sub-crystals (Figure 6d). Many sub-crystals appeared, but did not reach the temperature of complete recovery.

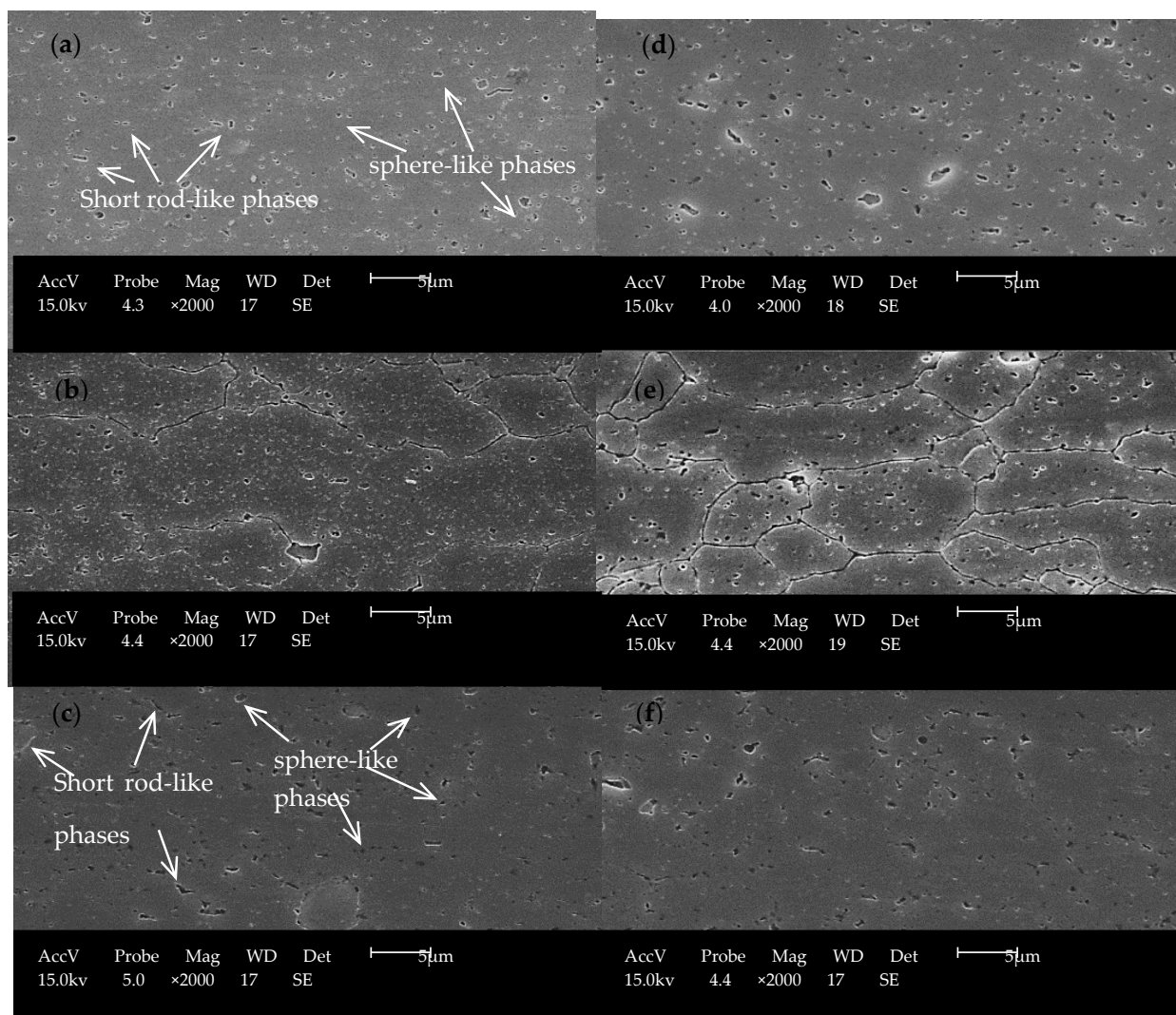


Figure 5. SEM images showing the morphology of the strip reinforcement plate under SEM. (a) 10%-110 °C/2 h; (b) 10%-220 °C/2 h; (c) 14%-110 °C/2 h; (d) 14%-220 °C/2 h; (e) 18%-110 °C/2 h; (f) 18%-220 °C/2 h.

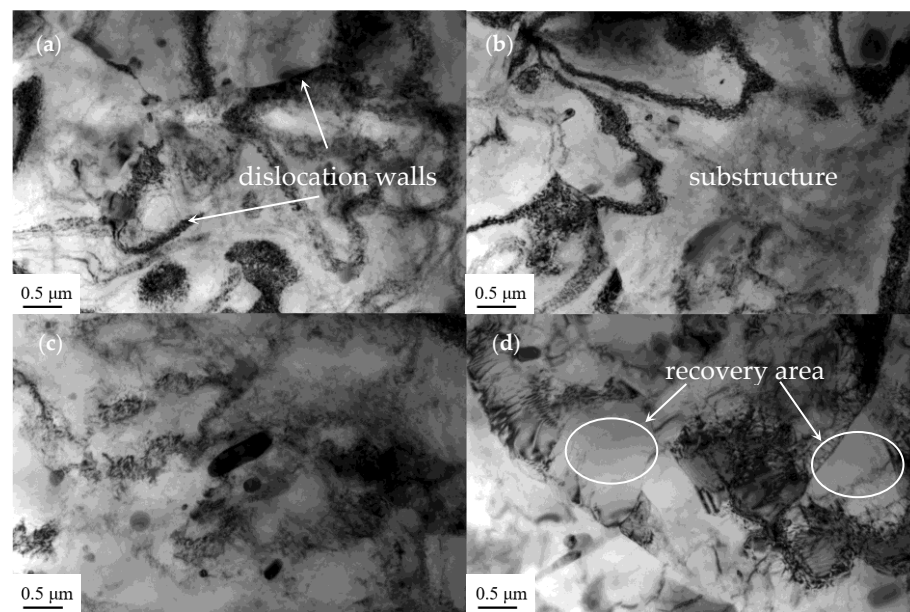


Figure 6. TEM image showing dislocation structures of the strip reinforcement plate after annealing at different temperatures. (a) 14%-120 °C/2 h; (b) 14%-220 °C/2 h; (c) 14%-300 °C/2 h; (d) 14%-360 °C/2 h.

4. Discussions

Intergranular corrosion sensitivity mainly depends on the characteristics of the precipitation phase at the grain boundary. The grain boundary has high interfacial energy, which is the main enrichment of impurities and alloying elements. In the aging process, solute atoms tend to diffuse to places of high interfacial energy. In order to obtain a good intergranular corrosion performance, the grain boundary precipitation phase is largely spaced with intermittent distribution, cutting off the grain boundary continuous corrosion channel. When the Al-Mg-Mn extrusion strip plate stabilization anneals at 300 °C, the precipitation phase is intermittently distributed so that the corrosion phenomenon is not obvious.

When the Al-Mg-Mn extrusion strip plate pre-deformation occurs under 5% tension, with stabilization annealing at 300 °C for 2 h and sensitization at 150 °C for 10 h, continuous rope β phase precipitation approximately 18 nm in diameter can be observed in the grain boundary, as shown in Figure 7a. When the pre-deformation under tension increases to 14% and stabilization annealing is conducted at 220 °C for 2 h, some dislocations existed around the coarse scaled Al_6Mn particles, as displayed in Figure 7b. It is also indicated that the Al_6Mn particles can hinder the dislocation degradation in the aging process and alleviate the reduction of strength caused by dislocation degradation. Compared to Figure 7a, a large number of continuous rope-like β -phase appeared on the grain boundary, and the diameter of the rope-like phase is about 19 nm. There are also slate-like and sphere-like phases precipitated near the grain boundary. Dislocation walls can also be observed as marked by the white dashed lines in Figure 7c. These contribute to the formation of subregions and refinement of the microstructure. When sensitization occurs at 150 °C for 50 h, it can be found that a continuous rope-like β -phase with an uneven diameter can be precipitated on the grain/subgrain boundaries (see Figure 7d). In addition, the diameter of a fine, rope-like precipitated phase can reach about 15 nm, and the diameter of a coarse, rope-like precipitated phase can reach about 40 nm. After stabilization annealing at 300 °C for 2 h and sensitization at 150 °C for 100 h, the β -phase is mostly intermittently distributed (Figure 7e), and the grain boundary precipitation phase gradually agglomerates into an intermittent coarse phase from the slender intermittent distribution, as the sensitization time increases. Pre-deformation under tension between 5–15% and grain boundary precipitation of the β -phase above 260 °C will not show continuous distribution at the grain boundary.

Intergranular corrosion performance is good, and when the annealing temperature is between 150–220 °C, β -phase precipitation occurs in the large grain boundary area. The Al-Mg-Mn alloy extruded strip reinforcement plate in the intergranular corrosion test shows a surface layer peeling phenomenon. From the above analysis, it is easy to see that the precipitation state of β -phase in high Mg aluminum alloys is the main factor affecting the intergranular corrosion performance. The continuous distribution of β -phase on the grain boundary will also significantly deteriorate the Al-Mg-Mn intergranular corrosion performance. The intergranular precipitation phase grows with the increase in aging time, and the precipitation phase will change from a continuous precipitation state to an intermittent precipitation state. Therefore, when the temperature reaches a certain value, the precipitation-free zone (PFZ) widens as the temperature increases. This reduces the continuity of the precipitated phase, and thus increases the corrosion resistance of the alloy [26,27]. The intergranular corrosion resistance of the alloy improves as the aging time increases.

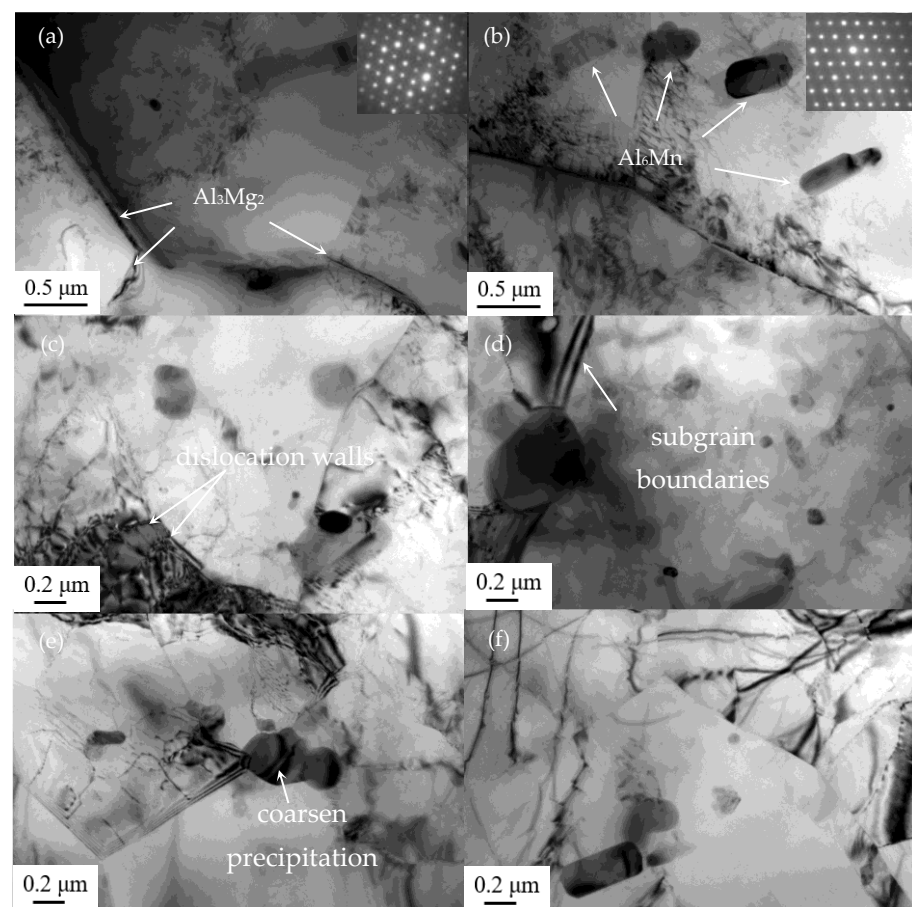


Figure 7. TEM images showing microstructures of strip reinforcement plate after sensitization at 150 °C. (a) 5%-300/2 h + 150 °C/10 h; (b) 14%-220/2 h + 150 °C/10 h; (c) 14%-300/2 h + 150 °C/10 h; (d) 14%-300/2 h + 150 °C/50 h; (e) 14%-300/2 h + 150 °C/100 h; (f) 14%-300/2 h + 150 °C/200 h.

5. Conclusions

In this work, the effects of the pre-deformation under tension and the annealing process on the microstructure and properties of Al-6Mg-1.0Mn extruded wide reinforcing plates were quantitatively investigated. The major results were as follows:

1. When the pre-deformation under tension is 10–14%, the corrosion resistance of the Al-Mg-Mn extruded ribbed plate increases with the increase in the annealing temperature. When the stabilization treatment temperature is in the range of 220–360 °C, the corrosion performance is first decreased, and then increases with the rise in tempera-

ture and becomes stable at 300 °C. After stabilization annealing at 300 °C for 2 h and sensitization at 150 °C, the resistance to intergranular corrosion is first decreased, and then increases with prolonged sensitization time.

2. The pre-deformation under tension and annealing process can regulate the interaction between dislocations and precipitates effectively, which improves the hardening effect and intergranular microstructure of the investigated alloy. The continuous distribution of β -phase at the grain boundaries significantly deteriorates the Al-Mg-Mn intergranular corrosion performance. The intergranular precipitation phase grows with the increase in sensitization time, and the precipitation phase changes from a continuous to intermittent precipitation state.
3. The pre-deformation under tension and the annealing process can, evidently, improve the mechanical properties of Al-Mg-Mn alloy. When the pre-stretching deformation amount is 14%, and stabilization annealing occurs at 300 °C for 2 h, the peak tensile strength of the alloy is 360 MPa, the yield strength is 205 MPa, and the elongation is 18.5%.

Author Contributions: Conceptualization, M.J., C.L., J.C. and X.W.; methodology, P.L.; validation, P.L.; formal analysis, P.L.; investigation, P.L.; resources, M.J., C.L., J.C. and X.W.; data curation, P.L.; writing—original draft preparation, P.L.; writing—review and editing, P.L., Q.H., W.S., P.L. and R.W.; supervision, M.J., C.L., J.C. and X.W.; project administration, M.J., C.L., J.C. and X.W.; funding acquisition, M.J., C.L., J.C. and X.W. All authors have read and agreed to the published version of the manuscript.

Funding: This research was funded by the Fundamental Research Funds for the National Natural Science Foundation of China (52271094, U1708251); and the Liaoning Revitalization Talents Program, China (XLYC1807027).

Data Availability Statement: The data presented in this study are available upon request.

Conflicts of Interest: The authors declare no conflict of interest.

References

1. Filatov, Y.A.; Yelagin, V.I.; Zakharov, V.V. New Al-Mg-Sc alloys. *Mat. Sci. Eng. A* **2000**, *280*, 97–101. [\[CrossRef\]](#)
2. Kaibyshev, R.; Musin, F.; Lesuer, D.R.; Gniew, T. Superplastic behavior of an Al-Mg alloy at elevated temperatures. *Mat. Sci. Eng. A* **2003**, *342*, 169–177. [\[CrossRef\]](#)
3. Zhang, R.; Knight, S.P.; Holtz, R.L.; Goswami, R.; Davies, C.H.J.; Birbilis, N. A survey of sensitization in 5xxx series aluminum alloys. *Corrosion* **2016**, *72*, 144–159. [\[CrossRef\]](#)
4. Wen, W.; Zhao, Y.; Morris, J.G. The effect of Mg precipitation on the mechanical properties of 5xxx aluminum alloys. *Mater. Sci. Eng. A* **2005**, *392*, 136–144. [\[CrossRef\]](#)
5. Zhang, X.M.; Nie, Z.R.; Huang, H.; Weng, S.P.; Gao, K.Y. Effect of cold deformation and annealing on intergranular corrosion property of 5E06 aluminium alloy plates. *T. Nonferr. Metal. Soc.* **2013**, *11*, 3056–3063.
6. Lee, B.H.; Kim, S.H.; Park, J.H.; Kim, H.W.; Lee, J.C. Role of Mg in simultaneously improving the strength and ductility of Al-Mg alloys. *Mater. Sci. Eng. A* **2016**, *657*, 115–122. [\[CrossRef\]](#)
7. Yin, Z.M.; Zhu, D.P.; Jiang, F. Recrystallization of Al-Mg-Mn and Al-Mg-Mn-Sc-Zr Alloys. *J. Mater.* **2004**, *6*, 3–6.
8. Li, Y.J.; Arnberg, L. Solidification structures and phase selection of iron-bearing eutectic particles in a DC-cast AA5182 alloy. *Acta Mater.* **2004**, *52*, 2673–2681. [\[CrossRef\]](#)
9. Jin, T.N.; Nie, Z.R.; Xu, G.F.; Ruan, H.Q.; Yang, J.J.; Fu, J.B.; Zuo, T.Y. Effects of cooling rate on solidification behavior of dilute Al-Sc and Al-Sc-Zr solid solution. *T. Nonferr. Metal. Soc.* **2004**, *14*, 58–62.
10. Guo, C.; Zhang, H.T.; Li, S.S.; Chen, R.X.; Nan, Y.F.; Li, L.; Wang, P.; Li, B.M.; Cui, J.Z.; Nagaumi, H. Evolution of microstructure, mechanical properties, and corrosion behavior of Al-4Mg-2Zn-0.3Ag (wt.%) alloy processed by T6 or thermomechanical treatment. *Corros. Sci.* **2021**, *188*, 109551. [\[CrossRef\]](#)
11. Guo, C.; Zhang, H.T.; Zou, J.; Li, B.M.; Cui, J.Z. Effects of pre-treatment combining with aging on the microstructures and mechanical properties of Al-Mg-Ag alloys. *Mater. Sci. Eng. A* **2019**, *740–741*, 82–91. [\[CrossRef\]](#)
12. Zuo, J.Z.; Hou, L.G.; Shi, J.T.; Zhuang, L.Z.; Zhang, J.S. The mechanism of grain refinement and plasticity enhancement by an improved thermomechanical treatment of 7055 Al alloy. *Mater. Sci. Eng. A* **2017**, *702*, 42–52. [\[CrossRef\]](#)
13. Vaseghi, M.; Kim, H.S. A combination of severe plastic deformation and ageing phenomena in Al-Mg-Si Alloys. *Mater. Des.* **2012**, *36*, 735–740. [\[CrossRef\]](#)
14. Nie, B.; Yin, Z.M.; Jiang, F.; Jiang, C.L.; Cong, F.G. Influence of stabilizing annealing on tensile property and exfoliation corrosion resistance of Al-Mg-Sc alloy. *Met. Sci. Heat Treat.* **2008**, *29*, 58–61.

15. Oguocha, I.N.A.; Adigun, O.J.; Yannacopoulos, S. Effect of sensitization heat treatment on properties of Al-Mg alloy AA5083-H116. *J. Mater. Sci.* **2008**, *43*, 4208–4214. [[CrossRef](#)]
16. Zhang, R.; Zhang, Y.; Yan, Y.; Thomas, S.; Davies, C.H.J.; Birbilis, N. The effect of reversion heat treatment on the degree of sensitisation for aluminium alloy AA5083. *Corros. Sci.* **2017**, *126*, 324–333. [[CrossRef](#)]
17. Lin, Y.K.; Wang, S.H.; Chen, R.Y.; Hsieh, T.S.; Tsai, L.; Chiang, C.C. The Effect of Heat Treatment on the Sensitized Corrosion of the 5383-H116 Al-Mg Alloy. *Materials* **2017**, *10*, 275. [[CrossRef](#)]
18. Tzeng, Y.C.; Lin, C.H. Effects of stabilization treatment on the precipitation behavior of β phase and stress corrosion for AA5383-H15 alloys. *J. Mater. Res.* **2019**, *34*, 2554–2562. [[CrossRef](#)]
19. Searles, J.L.; Gouma, P.I.; Bucheit, R.G. Stress corrosion cracking of sensitized AA5083 (Al-4.5Mg-1.0Mn). *Metall. Mater. Trans. A* **2001**, *32*, 2856–2867. [[CrossRef](#)]
20. Jones, R.H.; Baer, D.R.; Danielson, M.J.; Vetrano, J.S. Role of Mg in the stress corrosion cracking of an Al-Mg alloy. *Metall. Mater. Trans. A* **2001**, *32*, 1699–1711. [[CrossRef](#)]
21. Goswami, R.; Spanos, G.; Pao, P.S.; Holtz, R.L. Microstructural evolution, and stress corrosion cracking behavior of Al-5083. *Metall. Mater. Trans. A* **2011**, *42*, 348–355. [[CrossRef](#)]
22. ASTM G67; ASTM: G67–04 Standard Test Method for Determining the Susceptibility to Intergranular Corrosion of 5XXX Series Aluminum Alloys by Mass Loss After Exposure to Nitric Acid (NAML Test). ASTM International: West Conshohocken, PA, USA, 2004.
23. GB/T 7998; Intergranular Corrosion Test Method of Aluminium Alloy. 2005. Available online: <https://www.chinesestandard.net/PDF.aspx/GBT7998-2005> (accessed on 6 September 2022).
24. Najjar, D.; Magnin, T.J.; Warner, T.J. Influence of critical surface defects and localized competition between anodic dissolution and hydrogen effects during stress corrosion cracking of a 7050-Aluminium alloy. *Mater. Sci. Eng. A* **1997**, *238*, 293–302. [[CrossRef](#)]
25. Su, J.X.; Zhang, Z.; Cao, F.; Zhang, J.Q.; Cao, C.N. Review on the Intergranular Corrosion and Exfoliation Corrosion of Aluminum Alloys. *J. Chin. Soc. Corr. Pro.* **2005**, *25*, 187–192.
26. Chen, K.H.; Huang, L.P.; Zheng, Q.; Hu, H.W. Effect of high-temperature pre-precipitation on stress corrosion cracking of 7A52 alloy. *T Nonferr. Metal. Soc.* **2005**, *3*, 5.
27. Li, H.; Pan, D.Z.; Wang, Z.X.; Zheng, Z.Q. Influence of T6I6 Temper on Tensile and Intergranular Corrosion Properties of 6061 Aluminum Alloy. *Acta Metall. Sin.* **2010**, *46*, 494–499. [[CrossRef](#)]